Experiments in Fluids 9, 121–128 (1990)

Experiments in Fluids

Boundary layer diagnostics by means of an infrared scanning radiometer

L. de Luca and **G. M. Carlomagno**

Facoltà di Ingegneria, Università di Napoli, Piazzale Tecchio, 80, I-80125 Napoli, Italia

G. Buresti

Dipartimento di Ingegneria Aerospaziale, Università di Pisa, Via Diotisalvi, 2, I-56126 Pisa, Italia

Abstract. A computerized infrared (IR) scanning radiometer is employed to characterize the boundary layer development over a model wing, having a Göttingen 797 cross-section, by measuring the temperature distribution over its heated surface. The Reynolds analogy is used to relate heat transfer measurements to skin friction. The results show that IR thermography is capable of rapidly detecting location and extent of transition and separation regions of the boundary layer over the whole surface of the tested model wing. Thus, the IR technique appears to be a suitable and effective diagnostic tool for aerodynamic research in wind tunnels.

List of symbols

c	airfoil chord
c_f	local skin friction coefficient $= 2\tau/(\varrho V^2)$
c_p	specific heat coefficient at constant pressure
h	local convective heat transfer coefficient
Nu	Nusselt number $= h x/\lambda$
Nu_c	Nusselt number based on airfoil chord $= h c/\lambda$
Pr	Prandtl number $c_p \mu/\lambda$
Q_j	wall heat flux due to Joule heating
Q_l	heat flux loss
Re	Reynolds number $\varrho V x/\mu$
Re_c	Reynolds number based on airfoil chord $= \varrho V c/\mu$
St	Stanton number $= h/\varrho c_p V$
T_w	wall temperature
T_{aw}	adiabatic wall temperature
V	velocity of the free stream
x	chordwise spatial coordinate
α	angle of attack
λ	thermal conductivity coefficient
μ	dynamic viscosity coefficient
ϱ	mass density
τ	wall shear stress

1 Introduction

The performance of an airfoil, and in particular its effectiveness as a low-drag lift generating device, is strongly affected by the development of the boundary layer over its surface. Therefore, it is very important that experimental investigation tools be available for a quick detection of the location and extent of the regions where transition between laminar and turbulent flow, or separation of the boundary layer, take place for different values of the angle of attack and Reynolds number.

Transition and separation are often detected by means of intrusive probes in wind tunnel facilities. The interference effects induced in the flow field by the probes are one of the major causes which may invalidate the accuracy of the experimental measurements. This problem becomes particularly critical in low Reynolds number testing, due to the extreme sensitivity of the boundary layer to Reynolds number, pressure gradient and disturbance environment (Mueller et al. 1983). Hot film systems are also used for detecting transition (Bobbitt et al. 1985), whereas the location of separation is often determined from pressure distribution measurements (Ostowari 1987).

Surface flow visualization techniques can be a useful means for estimating the interaction of a fluid flow with the surface of a solid body (Merzkirch 1987). In general, the surface is coated with a thin layer of a "foreign" material which, upon interaction with the fluid flow, develops a certain visible pattern. Three different interaction processes are known which deliver different kinds of information: (i) mechanical interaction, which visualizes the surface flow and permits an evaluation of skin friction or, at least, of the direction of the wall tangential stresses. Various techniques are available: smoke wire (Batill and Mueller 1981) or direct injection (Freymuth et al. 1985; Mueller et al. 1987); oil film (Settles and Teng 1983); wall tufts; ii) surface mass transfer, which measures the mass transfer of a sublimating substance (Tien and Sparrow 1979; Marchman and Abtahi 1985); (iii) thermal interaction, which measures the heat transfer or surface temperature. Temperature-sensitive paints (e.g. for high enthalpy flows, Ceresuela et al. 1965) or liquid crystals (Cooper et al. 1975) have been used.

It is believed that the observed pattern can indicate the positions of transition in the wall boundary layer and of flow separation and reattachment. The question arises as to the interpretation and reliability of these observations, because the presence of the foreign material affects the boundary conditions for the air flow near the solid wall.

The Infrared Scanning Radiometer (IRSR) represents an effective investigation tool in convective heat transfer, in both steady state and transient techniques. Carlomagno and de Luca (1987, 1989) discussed the possibility of applying a computerized IR imaging system to measure convective heat transfer coefficients in a variety of physical situations where different data reduction methods may be used.

In principle the use of IRSR may be assigned to the class of techniques measuring the thermal interaction between a stream and a solid surface, although a foreign material is not present in this case. The essential features of the IR camera method are: it is non-intrusive; it yields a complete two-dimensional mapping of the surface to be tested; the video signal output may be treated by digital image processing.

As far as the application of the IRSR in boundary layer diagnostics is concerned, it is relatively simpler when the kinetic heating is large (Bynum et al. 1976; Carlomagno et al. 1989), i.e. when the stream Mach number is high (passive heating mode). Conversely, at low Mach numbers the kinetic heating is not sufficiently large to achieve a good thermal sensitivity, so that an active heating technique must be used. Monti and Zuppardi (1987) and Heath et al. (1987) employed transient techniques, by heating the model before testing and by using a CO_2 laser beam, respectively. Quast (1987) applied the infrared technique to qualitatively detect transition in different wind tunnels and in free flight experiments.

In the present work the potential of IR thermography for the experimental evaluation in a subsonic wind tunnel of the boundary layer development over model wings is analysed with the aid of a steady state procedure referred to as heated thin foil.

2 Thermal model

The possibility of evaluating the behaviour of the boundary layer over the surface of a body immersed in a flow by means of heat transfer measurements derives from the close relation existing between skin friction and heat flux at the wall. In the very simple case of a flat plate at zero incidence, under the assumption of laminar flow, constant wall temperature and unit Prandtl number, the classical Reynolds analogy yields

$$c_f = 2\,St \tag{1}$$

where

$$c_f = 2\,\tau/(\varrho\,V^2) \tag{2}$$

is the wall friction coefficient and

$$St = h/(\varrho\,c_p\,V) = Nu/(Re\,Pr) \tag{3}$$

is the Stanton number. *Nu*, *Re* and *Pr* are the Nusselt, Reynolds and Prandtl numbers, respectively.

In more general cases, such as compressible and incompressible flows around shaped bodies, and laminar and turbulent boundary layers, the validity of the Reynolds analogy may be open to criticism, particularly for flows at high Mach number (Fernholz and Finley 1980). Nevertheless, a "Reynolds analogy factor"

$$s = c_f/(2\,St) \tag{4}$$

may be introduced, and its value is found to be approximately constant and sufficiently close to unity for a wide variety of conditions, especially in the case of subsonic flows.

In contrast to the decreasing trend typical of attached laminar or turbulent flow, the regions of separated flow are characterized by a practically constant value of c_f, whereas the transition from laminar to turbulent boundary layer is accompanied by a significant increase in the wall friction coefficient. Therefore, the knowledge of the surface distribution of the convective heat transfer coefficient can certainly be utilized to obtain a rapid qualitative analysis of the state of the boundary layer over the body surface. Quantitative estimates of the skin friction coefficient may also be made, provided the necessary caution is exerted when applying the Reynolds analogy to the particular case under investigation.

In order to evaluate the convective heat transfer coefficient by means of an IR camera, a convenient procedure under steady state conditions is the heated thin foil technique. This method consists of heating by Joule effect a thin metallic foil coating the model surface and measuring the convective heat transfer coefficient, defined as

$$h = (Q_j - Q_l)/(T_w - T_{aw}) \tag{5}$$

where Q_j is the Joule heating per unit area, Q_l is the heat loss (including radiation and internal conduction), T_w is the temperature of the wall and T_{aw} is the adiabatic wall temperature of the flow.

Radiation may be minimized if the foil is heated at relatively low temperatures, which may be achieved if an IR scanner with a good thermal sensitivity is used. Low heat fluxes are also mandatory in order to avoid disturbances of the boundary layer structure over the body surface. Conduction from the foil to the inside of the model is negligible if the model itself is constructed with a thin layer of a low thermal conductivity material, such as epoxy, backed up by a thermal insulator. Being these conditions fulfilled, even the tangential conduction errors are very small due to the thinness of the foil.

By using an IRSR, the map of constant temperature lines may be recorded, and the heat flux distribution over the foil computed. In particular, if a boundary condition of constant heat flux (including heat losses) is achieved, each isotherm corresponds to a locus of constant heat transfer coefficient.

3 Experimental procedure

Tests are carried out in the subsonic wind tunnel of the Department of Aerospace Engineering of the University of Pisa, which is a Göttingen type, closed-return tunnel, with a

circular open test section 1.1 m in diameter and 1.48 m in length. The velocity of the flow may be continuously varied between 10 and 35 m/s. The model is vertically placed above a plate and connected with a six-component balance which is placed beneath the plate and sheltered by a NACA 0018 fairing. The balance is mounted on a rotatable base, which allows the model to be positioned at different angles of attack relative to the flow. The turbulence level of the stream, which is approximately 0.9%, is relatively high and corresponds to a Reynolds magnification factor of 1.75.

A low aspect ratio rectangular model wing, with a chord and a span of 0.18 m and 0.32 m, respectively, and a Göttingen 797 constant cross-section, is used in performing the tests. In order to improve the two-dimensional character of the flow around the airfoil, a 0.25 m wide, 0.5 m long, end plate, supported by the probe traversing mechanism of the wind tunnel, is placed at a distance of less than 1 mm from the model tip.

Two versions of the model are tested. The first one is made of solid Ureol 450, an easily-machinable synthetic resin with density similar to wood; the other one is made of a 3 mm thick layer of fiberglass epoxy over a polyurethane foam so as to check the influence of the internal conduction effect. Both models have 5 mm thick copper ribs at their tips. The leeside surface of each model is coated with a stainless steel foil, glued to the surface by means of epoxy resin. The coating foil (155 mm wide and 0.030 mm thick) starts 13 mm from the leading edge, covers the whole span of the models and is welded to the copper ribs in order to assure a low local electrical resistance. To enhance the thermal image detection by the IR camera and to reduce the effects of reflection from neighboring surfaces, the coating foil is blackened by means of a very thin film of black paint so as to achieve an emissivity coefficient approximately equal to 0.95.

With regard to the measurement of the adiabatic wall temperature, this latter is assumed to coincide with the temperature exhibited by the foil when Joule heating is suppressed. Hence, each test run consists of two parts. In the first one, the cold image of the foil is recorded to obtain T_{aw}; the surface temperature distribution T_w is then measured from the hot image which is obtained when the electrical current is heating the foil. The distribution of the temperature difference $T_w - T_{aw}$ is directly computed by subtracting the two digitized data matrices corresponding to these two thermal images. Due to the very low Mach number, in the present case T_{aw} practically coincides with the free stream static temperature. Typical heat fluxes are of the order of 7×10^{-2} W/cm^2.

The models are normally tested at a Reynolds number based on the wing chord $Re_c = 2.59 \times 10^5$, and at angles of attack α ranging from $-12°$ to $20°$. For an angle of attack of $-4°$, tests are also performed at Reynolds numbers of 1.52, 3.0 and 3.56×10^5. A few tests are also carried out with a transition trip (a 1 mm wide strip of grit N. 60 emery cloth) placed all along the wing span at approximately 28% of the chord from the leading edge.

The employed IR imaging system includes an AGEMA 782 Thermovision camera, an A/D converter Data Link, a BMC IF 800 computer with colour display, and a calibration unit. The acquisition and preliminary handling of the colour thermal image is carried out by means of a system software. Applicative software is developed to correlate measured temperatures to heat transfer coefficients and to present final results in graphic form. IR data are generally processed after proper numerical filtering and averaging. The digitized thermogram consists of a matrix of 128×128 pixels and the modulation transfer function is such that a temperature step on the viewed surface is completely resolved within about 5 pixels.

4 Results

No significant differences in detecting transition and separation locations are found between the results obtained with the two models of different material. However, as far as the measured values of the heat transfer coefficient are concerned, the ones obtained with the Ureol model are on the average 20% higher than the ones relative to the fiberglass epoxy model, which will be generally reported herein. This finding confirms that the thin wall epoxy model is the best choice, since it allows to minimize the effects of internal heat conduction. Tests carried out with the transition trip are, however, performed with the Ureol model.

4.1 Flow visualizations

A series of thermograms referring to the hot image of the model upper surface recorded for a chord Reynolds number equal to 2.59×10^5 and different angles of attack is reported in Fig. 1 a–d. The chordwise direction is the horizontal one and wind comes from the right side. The surface shown in each picture is approximately 170×170 mm^2. The image is detected by using a $7° \times 7°$ IR lens at a viewing distance of about 1.5 m, thus obtaining a spatial resolution on the computer displayed image of the order of 0.75 pixels/mm. The measurement is carried out by setting the thermal range of the scanner to the value of $R = 10$, which corresponds to a range of measured temperatures of about 15 °C.

In particular, Fig. 1 a shows the temperature field in the central region of the airfoil upper surface at an angle of attack of $-4°$. Free stream temperature is equal to 17.4 °C. The chordwise temperature variation is visualized by the sequence of vertical bands of different colour. The boundaries between the sky-blue and dark-green bands, on both sides, correspond approximately to the edges of the heated foil. The sky-blue band, where temperature ranges from 18.7° to 19.8 °C, shows that, even in the portion of the airfoil which is not heated, the surface temperature is slightly higher than the free stream one. However, the heating upstream of the foil, mainly due to internal conduction within the epoxy layer, is much less than the one downstream of the

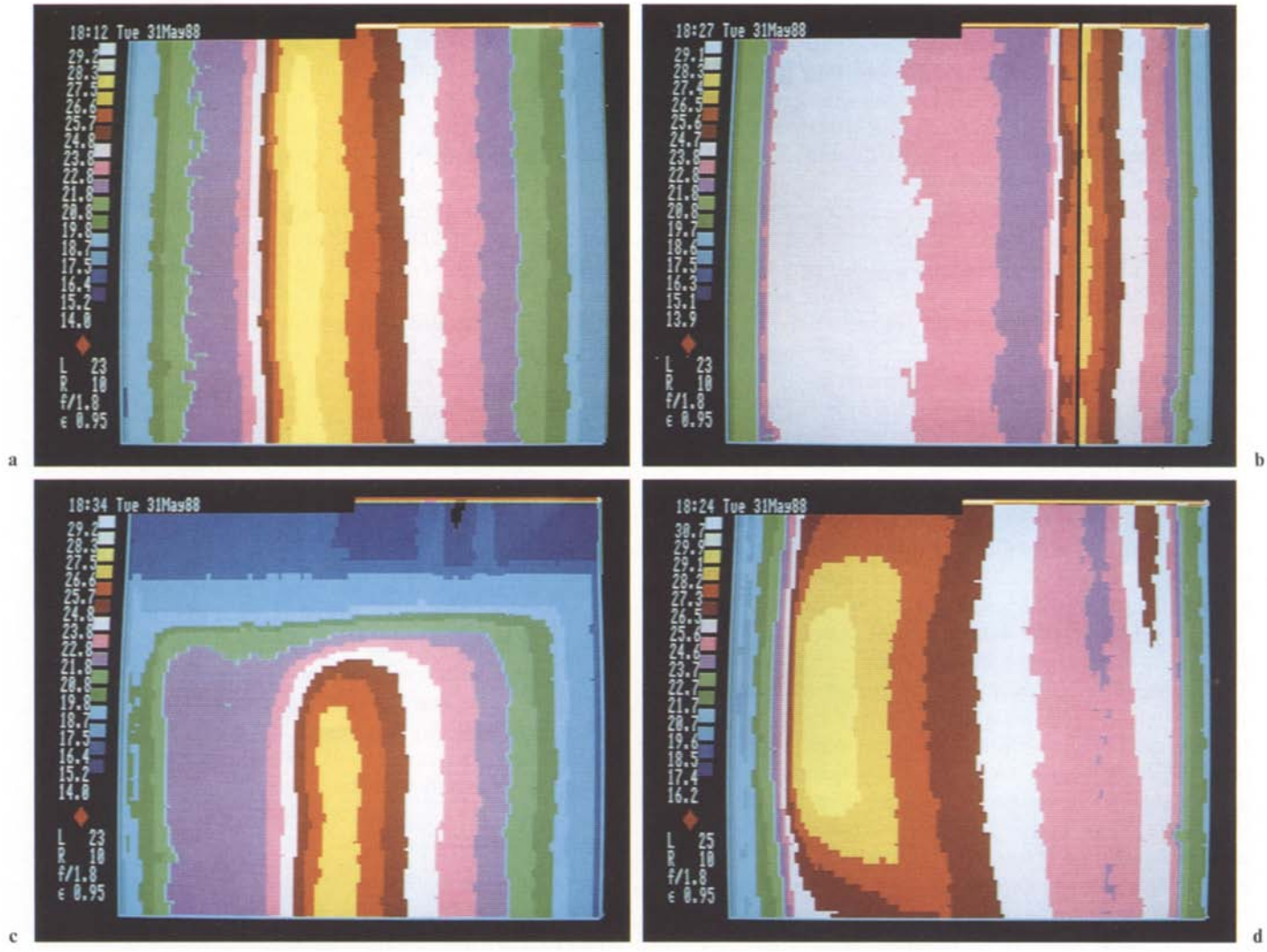

Fig. 1 a–d. Thermograms referring to the hot image of the airfoil leeside ($Re_c = 2.59 \times 10^5$): **a** $\alpha = -4°$, centerspan region, natural transition; **b** $\alpha = -4°$, centerspan region, with transition trip; **c** $\alpha = 0°$, airfoil upper tip, natural transition; **d** $\alpha = 20°$, centerspan region, natural transition

foil which is also affected by the hot boundary layer which is present before it.

The good two-dimensional character of the boundary layer in the present testing conditions is practically confirmed by the visualization of Fig. 1 a. The highest temperature level (i.e. lowest heat transfer coefficient) is attained in correspondence with the yellow zone. Downstream of the latter, the temperature decreases since transition to turbulent flow regime occurs in the boundary layer. As the cold image (not reported herein) shows a uniform surface temperature distribution, qualitative information on heat transfer coefficient (and then on flow conditions) may be directly drawn from this hot image. This occurrence practically applies to all the angles of attack tested.

Figure 1 b shows the thermogram obtained by placing a transition trip at 28% of the chord in the same testing conditions of the previous figure, except for the free stream temperature which is 18.5 °C. In this case the edges of the foil correspond approximately to the boundaries between the light green and violet bands. The position of the trip on the thermogram is indicated by the black line in the yellow zone which corresponds to the highest temperature, i.e. to the lowest heat transfer coefficient.

The transition induced by the trip is immediate and poses a severe challenge to the spatial resolution of the IR camera. In fact, downstream of the trip the temperature rapidly decreases as a consequence of the larger momentum and energy exchanges in the turbulent regime. The very high temperature gradient is visualized by the chordwise sequence of very narrow bands of different colour, from the yellow to the violet. Afterwards, the thickening of the boundary layer in the fully developed turbulent flow produces an increase of the temperature toward the trailing edge. Downstream of the minimum of temperature (located in the violet band), the

wide bands of uniform colour indicate a small change of the heat transfer coefficient there. The decrease of temperature in the very narrow pink and violet bands toward the trailing edge, corresponding to the foil edge adjacent to the unheated part of the model, is clearly due to conduction losses through the Ureol material. The comparison between Fig. 1 a and b gives an immediate appraisal of the abrupt change of the map of the lines of constant heat transfer coefficient when passing from natural to induced transition.

A thermogram recorded at zero angle of attack is reported in Fig. 1 c, where the region of the airfoil close to its upper tip is analysed in detail. Free stream temperature is 17.7 °C and the transition zone, which is present downstream of the yellow band, appears to be moved upstream with respect to the case of $\alpha = -4°$ (Fig. 1 a). It may be noted that the expected edge effects are limited within a very narrow region close to the model tip. This indicates that, even there, the constant heat flux boundary condition is achieved at a good level of accuracy; on the other hand, this same occurrence shows the relatively good two-dimensional character of the flow under these testing conditions.

On the contrary, the thermogram of Fig. 1 d, which is relative to the highest tested angle of attack ($\alpha = 20°$), shows a definite three-dimensional nature of the flow even in the airfoil centerspan region. The edges of the foil are located between the light green and violet bands. The latter is barely visible toward the trailing edge.

This picture clearly demonstrates the potential of IR thermography to evaluate the stalling characteristics of a wing in a complex three-dimensional situation. In the centerspan portion of the wing downward of the pink band, because of the fully turbulent boundary layer developing on the airfoil, the thermogram shows a chordwise continuous increasing of the temperature (except toward the foil trailing edge); accordingly, even at this large angle of attack the flow should be described as completely attached over the leeside, with the exception of the end of the foil. On the contrary, the upper and lower regions of the thermogram (i.e. toward the model tips) exhibit smaller changes of colour in a relatively wide region upstream of the trailing edge, indicating zones of practically constant temperature, i.e. constant heat transfer coefficient. By appealing to Reynolds analogy, this evidence means that a practically constant value of the skin friction occurs and therefore a separated flow regime is present.

4.2 Quantitative data

Fig. 2 a and b depict the chordwise centerspan variation of the Stanton number over the airfoil upper surface (leeside) for several angles of attack. For each x/c, the curves are obtained by averaging in the spanwise direction the data of the regions where the flow appears to be two-dimensional. The curves are defined over an interval of the chordwise abscissa x which is slightly shorter than the heated foil width because data referring to foil edges are cut off, being more influenced by the tangential conduction in the model wall.

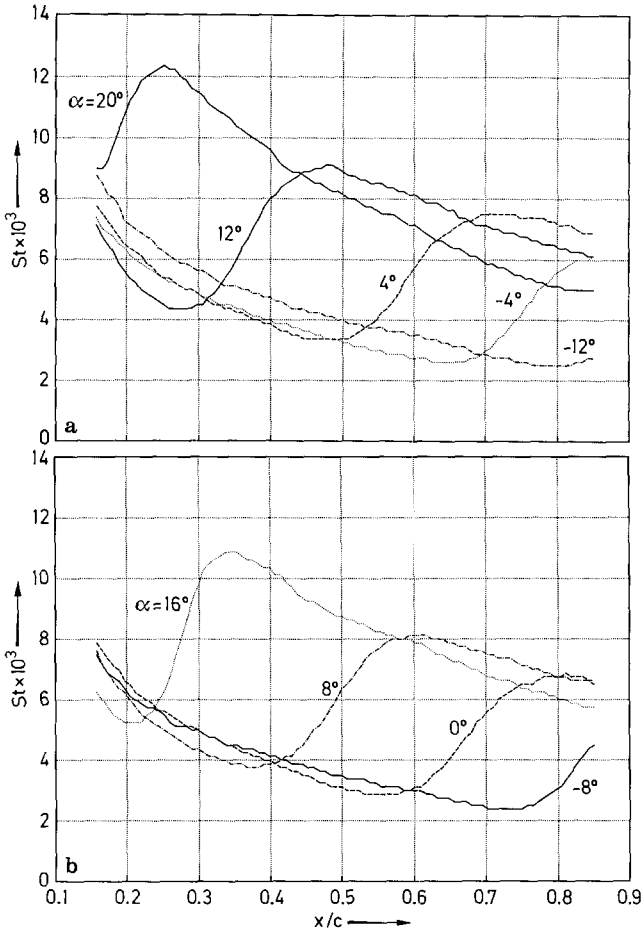

Fig. 2. a Chordwise distributions of local Stanton number over the leeside for several angles of attack ($Re_c = 2.59 \times 10^5$); **b** Chordwise distributions of local Stanton number over the leeside for several angles of attack ($Re_c = 2.59 \times 10^5$)

Within this interval, the evolution of the boundary layer from completely laminar to transitional and finally fully turbulent flow regimes as α is increased from $-12°$ to $20°$ is clearly apparent. In particular, the curve relative to $\alpha = -12°$ exhibits (except at high values of x/c) a monotonically decreasing trend of Stanton number which uncovers the similar behaviour of the wall friction coefficient in a laminar boundary layer with increasing distance from the forward stagnation point.

Around the minimum St value a plateau seems to occur in each curve. According to the description of Mueller et al. (1987), the location of the beginning of the plateau may be interpreted as the point of laminar separation and the plateau itself could be correlated to the laminar portion of a bubble, where the fluid moves very slowly. The end of the plateau instead may correspond to the beginning of transition in the separated shear layer. The subsequent rise of the Stanton number may be attributed to the turbulent flow regime developing in the so called turbulent portion of the bubble, where the flow vigorously moves in a recirculating pattern.

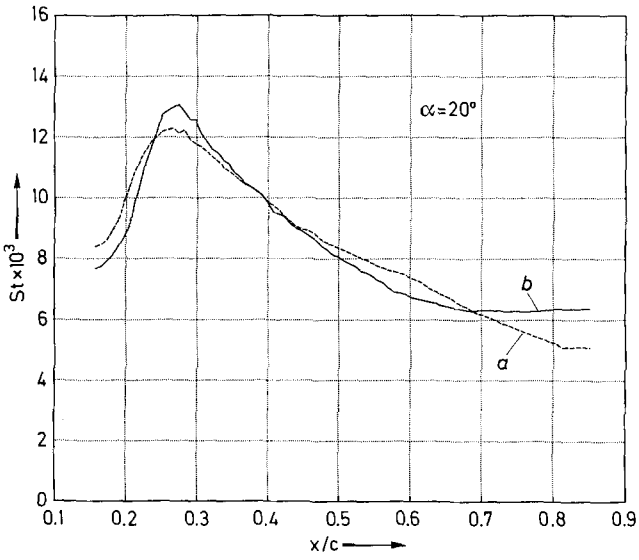

Fig. 3. Comparison between chordwise distributions of local Stanton number at centerspan and near the airfoil upper tip ($\alpha = 20°$; $Re_c = 2.59 \times 10^5$)

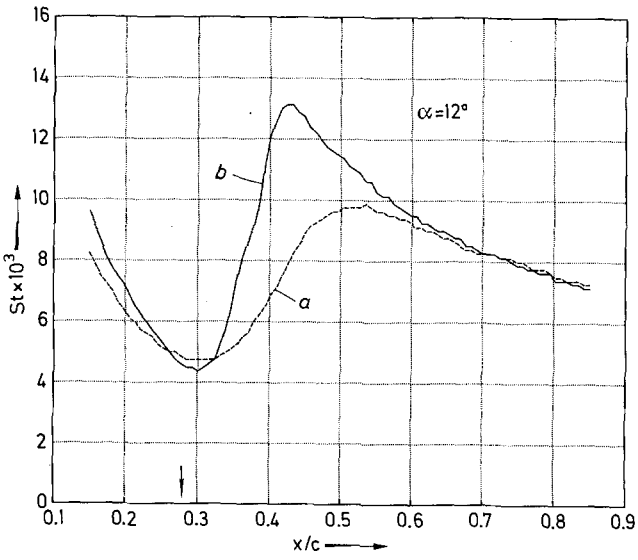

Fig. 4. Comparison between Stanton number distributions for natural transition and transition induced by a trip at 28% of the chord ($\alpha = 12°$; $Re_c = 2.59 \times 10^5$)

As α is progressively increased, the minimum St value moves upstream in agreement with the upstream movement of the laminar separation point which is exhibited by an airfoil as a consequence of the increase of the adverse pressure gradient on its leeside.

Starting from $\alpha = 4°$ a maximum St value is also clearly evident; this maximum may be correlated with the reattachment point (downstream edge of the separation bubble). Downstream of this maximum the beginning of a fully turbulent boundary layer, which is again characterized by a decrease of Stanton number (i.e. of the wall friction coefficient) along the chord, occurs.

In agreement with the typical characteristics of a separation bubble described by Arena and Mueller (1980), as the angle of attack increases the whole bubble moves toward the stagnation point and becomes shorter in length. Moreover, the extension of the laminar portion of the separated shear shortens, the St plateau practically disappearing at the highest α values. However, it has to be pointed out that in these cases the effects of a higher tangential conduction in the model wall (especially due to the steeper ascent of St in the turbulent portion of the bubble) and of the modulation transfer function of the IR scanner (MTF, which defines its spatial resolution) contribute to round off the curves around their minima and maxima.

The present data are in qualitative agreement with those of Render et al. (1986) which performed tests at $Re_c = 3 \times 10^5$. However, from a quantitative point of view, in the present finding the length of the bubble is longer and its location appears shifted downstream with respect to the data of Render et al. (1986). Furthermore, Render et al. find that turbulent separation occurs at high incidences. These discrepancies can be attributed, among other effects (such as a certain three-dimensionality of the flow and the small step on the airfoil surface due to the presence of the heating foil), to the relatively high turbulence level of the free stream.

For $\alpha = 20°$ present data show (except at the beginning of the foil and at very high values of x/c) a monotonic decrease of the wall heat transfer coefficient (fully turbulent boundary layer development) almost all over the metallic foil. It has to be pointed out that no significant plateau of constant Stanton number is noted upstream while St seems to be constant at the end of the foil. This latter finding may suggest the onset of a trailing edge turbulent separation at about 80% of the chord. It should be remembered that, as already pointed out, only some of the plots of Fig. 2 refer to spanwise averaged data. Although the two-dimensional character of the flow is enhanced by placing an end plate at the model upper tip, the thermograms reveal that the low aspect ratio of the wing has a significant effect on the aerodynamic field at high angles of attack ($\alpha > 14°$). This fact is proven in Fig. 3 where the St number distributions along the centerspan (curve a) and near the upper airfoil tip (curve b) are shown. As may be noted, in the zone near the wing tip St is practically constant downstream 67% of the chord, so that the turbulent boundary layer appears to be separated there.

The effect of artificially inducing transition by means of a trip placed on the leeside at 28% of the chord is shown in Fig. 4, where the distributions of the Stanton number obtained with (curve b) and without the transition trip (curve a) for $\alpha = 12°$ are reported. In these curves data are taken on the solid Ureol 450 model. Although the rapid rise of the Stanton number is affected by errors due to both conduction effects (which are greater for the solid model) and to the MTF of the system, it is evident that the triggering of transition is immediate. This result is confirmed by all the tests

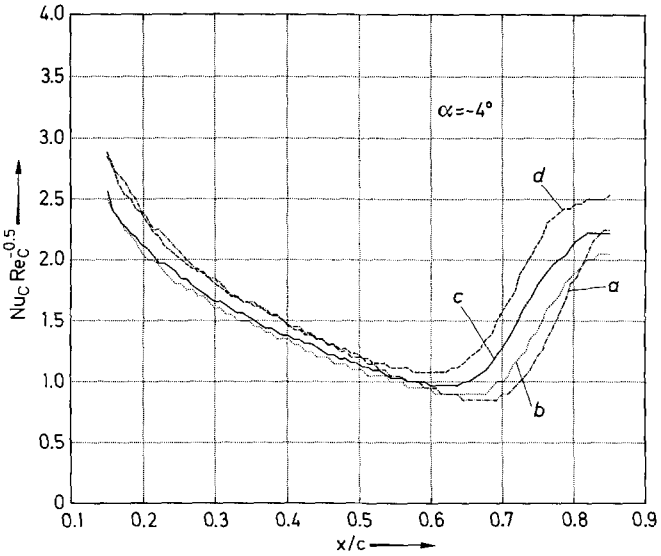

Fig. 5. Correlation of local chord Nusselt number distributions with chord Reynolds number ($\alpha = -4°$): **a** $Re_c = 1.52 \times 10^5$; **b** $Re_c = 2.59 \times 10^5$; **c** $Re_c = 3.0 \times 10^5$; **d** $Re_c = 3.56 \times 10^5$

performed in the range of incidences $-12° \leqq \alpha \leqq 12°$, where the onset of transition from laminar to turbulent flow is remarkably independent of the angle of attack.

The influence of the Reynolds number is shown in Fig. 5 where, for $\alpha = -4°$, the expected movement upstream of the transition point location is recovered. In agreement with the classical result of the laminar boundary layer theory, the quantity $Nu_c\,Re_c^{-0.5}$ appears to be essentially independent of Re_c and, before the separation bubble, it results within an acceptable approximation that:

$$Nu_c\,Re_c^{-0.5} \propto (x/c)^{-0.5} \tag{6}$$

5 Conclusions

Experimental tests are carried out which confirm the capability of an IR imaging system to investigate the boundary layer behaviour over a wing model tested in a subsonic wind tunnel at different flow conditions.

The heated thin foil technique is used to measure the convective heat transfer coefficient and the Reynolds analogy is used to relate measured convective heat transfer data to wall skin friction. The beginning and the extent of the laminar separation bubble and the location of turbulent reattachment points, as well as the regions where the turbulent boundary layer is separated, are quickly identified all over the leeside surface of the tested model wing even for the case of highly three-dimensional flow. However it is believed that, in order to detect the laminar separation bubble and the onset of the turbulent separation more precisely, a model having a thinner wall should be used so as to minimize the influence of the tangential heat flux.

The remarkable effectiveness of a strip of emery cloth in triggering transition in a very wide range of angles of attack is also clearly evident. Finally, by varying the Reynolds number, a confirmation is found of the expected upstream movement of the position of the boundary layer transition region and the law of laminar boundary layer development is recovered as well.

The soundness of the predictions yielded by the IRSR technique is corroborated by the results of flow visualizations with wall tufts. However, it has to be pointed out that, especially for the model made of solid resin, the results are affected by the tangential conduction effects in the model wall. This is particularly true for the case of rapidly varying temperature distributions. In this case attention should also be paid to the modulation transfer function defining the spatial resolution of the IR scanner. Anyhow, this latter may be varied by using a proper optic lens.

References

Arena, A. V.; Mueller, T. J. 1980: Laminar separation, transition, and turbulent reattachment near the leading edge of airfoils. AIAA J. 18, 747–753

Batill, S. M.; Mueller, T. J. 1981: Visualization of transition in the flow over an airfoil using the smoke-wire technique. AIAA J. 19, 340–345

Bobbitt, P. J.; Waggoner, E. G.; Harvey, W. D.; Dagenhart, J. R. 1985: A faster transition to laminar flow. SAE Tech. Paper 851855

Bynum, D. S.; Hube, F. K.; Key, C. M.; Diek, P. M. 1976: Measurement and mapping of aerodynamic heating with an infrared camera. AEDC Rept. TR-76-54, pp. 1–33

Carlomagno, G. M.; de Luca, L. 1987: Heat transfer measurements by means of infrared thermography. In: Flow visualization IV. (ed. Veret, C.). pp. 611–616. Washington: Hemisphere

Carlomagno, G. M.; de Luca, L. 1989: Infrared thermography in heat transfer. In: Handbook of flow visualization (ed. Yang, W. J.). pp. 531–553. Washington: Hemisphere

Carlomagno, G. M.; de Luca, L.; Alziary, T. 1989: Heat transfer measurements with an infrared camera in hypersonic flow. In: Computer and experiments in fluid flow (eds. Carlomagno, G. M.; Brebbia, C. A.). pp. 467–476. Berlin, Heidelberg, New York: Springer

Ceresuela, R.; Betremieux, A.; Caders, J. 1965: Mesure de l'échauffement cinétique dans les souffleries hypersoniques au moyen de peintures thermosensibles. Rech. Aérosp. 109, 13–19

Cooper, T. E.; Field, R. J.; Meyer, J. F. 1975: Liquid crystal thermography and its application to the study of convective heat transfer. J. Heat Transfer 97, 442–450

Fernholz, H. H.; Finley, H. A. 1980: A critical commentary on mean flow data for two-dimensional compressible turbulent boundary layers. AGARD AG-253

Freymuth, P.; Bank, W.; Palmer, M. 1985: Use of titanium tetrachloride for visualization of accelerating flow around airfoils. In: Flow visualization III. (ed. Yang, W. J.). pp. 99–105. Washington: Hemisphere

Heath, D. M.; Winfree, W. P.; Carraway, D. L.; Heyman, J. S. 1987: Remote non-contacting measurements of heat transfer coefficients for detection of boundary layer transition in wind tunnel tests. Proc. of ICIAFS '87. pp. 135–139. Williamsburg/VA

Marchman, J. F. III; Abtahi, A. A. 1985: Aerodynamics of an aspect ratio 8 wing at low Reynolds numbers. J. Aircraft 22, 628–634

Merzkirch, W. 1987: Flow visualization, 2nd edn. New York: Academic Press

Monti, R.; Zuppardi, G. 1987: Computerized thermographic technique for the detection of boundary layer separation. In: Aerodynamic data accuracy and quality: requirements and capabilities in wind tunnel testings. AGARD Conf. Preprint N. 429. pp. 30/1–15

Mueller, T. J.; Pohlen, L. J.; Conigliaro, P. E.; Jansen, B. J. 1983: The influence of free-stream disturbances on low Reynolds number airfoil experiments. Exp. Fluids 1, 3–14

Mueller, T. J.; Brendel, M.; Schmidt, G. S. 1987: Visualization of the laminar separation bubble on airfoils at low Reynolds numbers. In: Flow visualization IV. (ed. Veret, C.). pp. 359–364. Washington: Hemisphere

Ostowari, C. 1984: A rapid technique for measuring and visualizing the extent of separated flow. Exp. Fluids 2, 67–72

Quast, A. 1987: Detection of transition by infrared image technique. Proc. of ICIAFS '87, pp. 125–134. Williamsburg/VA

Render, P. M.; Stollery, J. L.; Williams, B. R. 1986: Aerofoils at low Reynolds numbers. Prediction and experiment. In: Numerical and physical aspects of aerodynamic flows III. (ed. Cebeci, T.). pp. 155–167. Berlin, Heidelberg, New York: Springer

Settles, G. S.; Teng, H. Y. 1983: Flow visualization methods for separated three-dimensional shock wave/turbulent boundary layer interactions. AIAA J. 21, 390–397

Tien, K. K.; Sparrow, E. M. 1979: Local heat transfer and fluid flow characteristics for airfoil oblique or normal to a square plate. Int. J. Heat Mass Transfer 22, 349–360

Received September 12, 1989